Nanoscale

PAPER

View Article Online
View Journal | View Issue

Check for updates

Cite this: *Nanoscale*, 2026, **18**, 918

Properties of AgNPs stabilized with polyvinylpyrrolidone relevant to antidiabetic agents

Victoria Vera Pineda, [a] Antonio Alvarez de la Paz, [b] Nina Bogdanchikova, *[c] Alexey Pestrykov, [d] Juan José Acevedo Fernández [e] and Maira Rubi Segura Campos *[a]

Received 14th August 2025,
Accepted 6th November 2025

DOI: 10.1039/d5nr03452c

rsc.li/nanoscale

Type 2 diabetes mellitus (DM2) is a chronic metabolic disease. Silver nanoparticles (AgNPs) show promise in their treatment. This study assessed the potential of AgNPs as DM2 treatment agent using *in vitro*, *in vivo*, and machine learning approaches. Male Wistar rats were used to study antihyperglycemic effects, while male mice evaluated hypoglycemic effects. *In vivo* studies showed that AgNPs inhibited α-amylase, α-glucosidase, and dipeptidyl peptidase-4, up to 3.51, 3827.76, and 11 times more effective than acarbose and sitagliptin, respectively. Advanced glycation end products inhibition by AgNPs was up to 61.4 times higher than metformin. *In vivo* experiments revealed that AgNPs antihyperglycemic activities were close to acarbose, while the same hypoglycemic effect was achieved with AgNP doses up to 167 times lower than that of glibenclamide. The results show the possibility to decrease the glibenclamide dose by two orders, that indicates high AgNP perspective to reduce drug toxicity and side effects.

Open Access Article. Published on 10 December 2025. Downloaded on 1/20/2026 10:49:24 PM.
This article is licensed under a Creative Commons Attribution 3.0 Unported Licence.

Introduction

DM2 is a chronic metabolic disease characterized by hyperglycemia leading to alterations in the secretion or action of insulin. In the long term, hyperglycemia induces oxidative stress due to the presence of reactive oxygen species (ROS). These ROS trigger tissue dysfunctions and increase the risk of micro- and macrovascular complications, such as hypertension, myocardial infarction, diabetic retinopathy, dyslipidemia, and diabetic nephropathy.[1,2] Currently, one of the focuses of pharmacological treatment for type 2 diabetes is the inhibition of enzymes involved in glucose metabolism, such as α-amylase and α-glucosidase, to slow down postprandial glucose fluctuations. In recent years, however, new therapeutic approaches have been investigated to restore glucose homeostasis and prevent underlying complications.[3–5] Among these approaches, the antidiabetic effect mediated by the inhibition of dipeptidyl peptidase-4 (DPP-4) glycoprotein has been suggested, thus improving the endogenous insulinotropic incretin. Another approach is to inhibit the formation of advanced glycation end products (AGEs), which promote reduced insulin resistance and the accumulation of ROS.[6]

Current pharmacotherapies decrease blood glucose, but they have limitations, including side effects and incomplete prevention of complications. This has led to a constant search for new therapeutic options that minimize the side effects and adverse reactions.[7] In the search for safe and effective biomedical alternatives, silver nanoparticles (AgNPs) have emerged as a potential treatment for diabetes mellitus. AgNPs have demonstrated therapeutic benefits in diabetes, such as improving wound healing in diabetic rabbits, attenuating endothelial dysfunction in diabetic rats, and reduce insulin resistance by regulating PI3K, insulin receptor, and glucose transporter 2 (GLUT2).[8,9]

The results of these studies underscore the need to develop AgNP formulations that balance high antidiabetic efficacy with low toxicity. Among them, Argovit™ AgNPs stabilized with polyvinylpyrrolidone (PVP) represent one of the appropriate candidates due to their reproducible synthesis, controlled physicochemical properties, and high stability in water solution (2 years).[10] Previous toxicological assessments reported LD_{50} values (calculated for AgNPs including metallic Ag and

[a]*Faculty of Chemical Engineering, Autonomous University of Yucatan (UADY), Merida 97300, Yucatan, Mexico. E-mail: victoriavera815@gmail.com, maira.segura@correo.uady.mx*
[b]*Materials Research Institute, National Autonomous University of Mexico (UNAM), Mexico City 04510, Mexico. E-mail: antonio.adlp@iim.unam.mx*
[c]*Center for Nanoscience and Nanotechnology (CNyN), Campus Ensenada, National Autonomous University of Mexico (UNAM), Mexico City 04510, Mexico. E-mail: nina@ens.cnyn.unam.mx*
[d]*Research School of Chemistry & Applied Biomedical Sciences, Tomsk Polytechnic University, Tomsk 634050, Russia. E-mail: pestryakov2005@yandex.ru*
[e]*Faculty of Medicine, Autonomous University of the State of Morelos (UAEM), Cuernavaca 62350, Morelos, Mexico. E-mail: juan.acevedo@uaem.mx*

This journal is © The Royal Society of Chemistry 2026

Open Access Article. Published on 10 December 2025. Downloaded on 1/20/2026 10:49:24 PM. This article is licensed under a Creative Commons Attribution 3.0 Unported Licence.

PVP) between 17 783 and 30 100 mg kg^{-1}, classifying them as "harmless" under OECD Guideline 420,[11] with no significant histopathological alterations or genotoxic effects.[12–14] Moreover, Argovit™ AgNPs showed low hemolytic activity and have been safely applied in humans for diabetic foot ulcers, tuberculosis, postoperative nasal infections, *etc.*[15–20] These attributes make them a standardized, safe, and biocompatible platform for evaluating their antidiabetic potential. Therefore, this study aimed to assess the *in vitro* and *in vivo* biological properties of five Argovit™ PVP-AgNP formulations as potential adjuvants for DM2 treatment, focusing on their inhibitory effects on α-amylase, α-glucosidase, DPP-4, and AGE formation, as well as their antihyperglycemic and hypoglycemic activities. This study, therefore, aimed to provide a preliminary assessment of the biological characteristics of PVP-functionalized Argovit AgNPs as potential adjuvants for DM2 treatment, considering their previously demonstrated wound-healing potential in diabetic patients.

Methods

AgNP formulations

Five AgNP formulations (abbreviated as Ag1–Ag5) belonging to the Argovit™ AgNP formulation family were provided by the Scientific and Production Center Vector-Vital Ltd (Novosibirsk, Russia). The synthetic processes, including the reduction of $AgNO_3$ by a high-energy electron beam, are detailed in patents RU 2.602.534 C2 and RU 2.602.741 C2. The characterization of the nanoparticles was previously published.[11] Briefly, AgNPs formulations contain 1.2, 18.8, and 80.0 wt% of metallic Ag, polyvinylpyrrolidone with different molecular masses (10–52 kDa), and distilled water, respectively. For all samples, silver particle size varies between 5–80 nm, with average ones lying in the range of 16–31 nm. *Z*-Potential lies in the range of −4.6–+5.1 mV (Table 1). The main difference in physicochemical properties of these samples was observed for hydrodynamic diameters, whose values varied by an order of magnitude (44–493 nm). All concentrations of AgNPs in the article were calculated for metallic Ag.

In vitro experiments

A-amylase and α-glucosidase inhibition assays. The inhibitory activity of AgNPs on α-amylase and α-glucosidase was measured using the method of Dineshkumar *et al.*[21] For α-amylase, starch (2 mg) was mixed with Tris-HCl buffer and $CaCl_2$ and incubated with AgNPs and α-amylase (0.211 mg mL^{-1}) at 37 °C for 10 minutes. The α-amylase activity was measured by a colorimetric method using a 3,5-dinitrosalicylic acid (DNS) reagent. Absorbance was measured post-DNS treatment. For α-glucosidase, 20 μL of α-glucosidase (0.2 mg mL^{-1}) and AgNPs were incubated (5 minutes at 37 °C), followed by 20 μL *p*-nitrophenyl-glucopyranoside (3.01 mg mL^{-1}), and reaction termination with 50 μL of sodium carbonate. The assay was performed in triplicate, and inhibition was calculated following eqn (1):

$$\%\ \text{inhibition} = \frac{(A_c{}^+) - (A_c{}^-) - (A_s - A_b)}{(A_c{}^+) - (A_c{}^-)} \times 100 \qquad (1)$$

where $A_c{}^+$ is the absorbance of the enzyme only, $A_c{}^-$ is the absorbance without enzyme, A_s is the absorbance with enzyme and the studied sample, and A_b is the blank absorbance.

The half-maximal inhibitory concentration (IC_{50}) values for the enzyme inhibition assays were calculated using non-linear regression analysis with inhibition data at different concentrations of AgNPs, using eqn (2):

$$IC_{50} = \frac{(50 - b)}{m} \qquad (2)$$

where b is the intersection, and m is the slope.

Mechanism of inhibition of α-glucosidase. The mechanism of inhibition of α-glucosidase by AgNPs was determined by plotting Lineweaver–Burk graphs based on the results of the assays described above. *p*-Nitrophenyl glucopyranoside (*p*-NPG) concentrations were 0.189, 0.376, 0.735, 1.506, 3.012 and 6.024 mg mL^{-1}. Two concentrations of AgNPs were used, corresponding to the IC_{10} and IC_{50}. The kinetic parameters were calculated according to Kan *et al.*[22]

Inhibition of dipeptidyl peptidase 4. DPP-4 inhibitory activity was determined using a fluorescence kit according to

Table 1 Physicochemical properties of five Argovit lots. The data were adapted from ref. 11

Properties	Ag-1	Ag-2	Ag-3	Ag-4	Ag-5
Average diameter of metallic cores ∅Ag (nm)	16.4 ± 8.0	25.4 ± 13.2	19.0 ± 9.3	16.4 ± 8.1	30.6 ± 23.2
TEM size distribution (nm)	5–40	5–60	5–40	5–40	5–80
PVP	K-15[a]	K-17[b]	K-17[b]	K-30[c]	12.6 kDa
Hydrodynamic diameter ∅hydro (nm)	448.7	90.4	43.8	483.2	121.1
Polydisoersity index (PDI)	0.813	0.270	0.433	0.555	0.280
Zeta potential ζ (mV)	−0.872	−4.56	+5.13	−0.464	−1.46
Surface plasmon resonance (λ, nm)	415	402, 444	402	406–549	429
TGA analysis of metallic silver (ω/ω%)	1.14 ± 0.02	1.32 ± 0.05	1.26 ± 0.03	1.19 ± 0.01	1.31 ± 0.01
PVP (ω/ω%)	19.62 ± 0.30	24.49 ± 0.70	24.43 ± 0.20	20.92 ± 0.42	21.67 ± 0.50
H_2O (ω/ω%)	79.24 ± 0.45	74.25 ± 0.60	75.74 ± 0.25	77.89 ± 0.80	77.02 ± 0.40
Morphology	Spherical	Spherical	Mostly spherical	Mostly spherical	Spherical

[a] K-15: 8–12 kDa. [b] K17: 10–16 kDa. [c] K-30: 45–58 kDa.

Open Access Article. Published on 10 December 2025. Downloaded on 1/20/2026 10:49:24 PM. This article is licensed under a Creative Commons Attribution 3.0 Unported Licence.

the manufacturer's specifications CS0002 (Sigma-Aldrich, St Louis, MO, EE. UU.).

Inhibition of advanced glycation products (AGEs). AGE inhibition was evaluated using the bovine serum albumin (BSA) – glucose model, Starowicz & Zieliński.[23] BSA (10 mg mL^{-1}) and glucose (90 mg mL^{-1}) were dissolved in phosphate buffer (pH 7.4). Then, 0.5 mL of each AgNP formulation was mixed with 0.5 mL of BSA and 0.5 mL of glucose. The blank solution contained 1 mL phosphate buffer, 1 mL BSA, and 1 mL glucose. Tubes were incubated in the dark for 48 hours at 37 °C. Fluorescence intensity was measured with a Cytation3 reader (Biotek®) at λ_{em} 420 nm and λ_{exc} 360 nm. AGE inhibition was calculated using eqn (3):

$$\%\,\text{inhibition} = \left(1 - \frac{FI_{AgNPs}}{FI_{blank}}\right) \times 100\% \quad (3)$$

where FI_{AgNPs} and FI_{blank} are the fluorescence intensity of AgNPs-containing and blank samples, respectively.

In vitro study data are represented as the mean value with standard deviation for three replicates. All optical measurements were performed by subtracting the spectrum of the corresponding AgNP control sample from the sample spectrum. Every AgNP control sample was the AgNP water solution with the same AgNP concentration as in the sample under study.

Correlation-based network analysis

A correlation-based network analysis was conducted to explore the relationships between the bioactivities of α-amylase, α-glucosidase, DPP-4, and AGE formation inhibition (IC_{50}), alongside their physicochemical characteristics.[24] The NetworkX library in Python 3.9 was used, employing the Spearman correlation method. The results were displayed as a correlation network, where green nodes represent physicochemical properties and orange nodes represent bioactivities. Edges indicate correlation scores, with node size reflecting the number of connections. Blue and red lines indicate positive (+) and negative (−) correlations, respectively, with line thickness representing the Spearman correlation coefficient (r).

Classification analysis based on principal component analysis (PCA)

The multivariate classification was based on the IC_{50} values of bioactivities. The AgNP sample with the highest inhibition potential for α-amylase, α-glucosidase, DPP-4, and AGE formation was set as the reference (100% activity). AgNP samples were categorized into three groups: high activity (>50% in four bioactivities), moderate activity (>50% in three), and low activity (>50% in one or two). Principal component analysis (PCA) was applied to normalize and visualize the relationship between physicochemical properties and bioactivities. The blue solid circles show a perfect correlation (r = 1.0) between components, and the red dotted circle indicates a moderate correlation (r = 0.5). The machine learning model and multivariate analysis were conducted using scikit-learn.[24]

This study represents a preliminary exploration of the antidiabetic potential of a specific AgNP formulation. Given the limited number of samples available, the classification model may be prone to overfitting. Future work will require a larger and more diverse dataset to improve model robustness and to identify which physicochemical properties are most relevant for optimizing the antidiabetic potential of AgNPs.

In vivo experiments

To assess antihyperglycemic activity, male Wistar rats aged 2–3 months, weighing 350–450 grams, were used. Male CD1 mice, 9 weeks old and weighing 25–30 grams, were employed for hypoglycemic activity. Animals were maintained under standard conditions with a 12-hour light/dark cycle at 23–25 °C and 50% humidity, with *ad libitum* access to food. All procedures adhered to the animal care guidelines of Directive 86/609/EEC and the "Mexican Official Standard NOM 062-ZOO-1999". Ethics approval was granted by the Institutional Animal Care and Use Committee (CCUAL-FM: 05/2016).

Oral glucose tolerance test (OGTT) in normal rats

The OGTT was determined according to Uuh–Narvaez *et al.*[25] Groups of six rats were fasted for 8 hours before receiving oral treatments *via* stainless-steel cannula. Negative control: starch (1 g kg^{-1}) to induce hyperglycemia. Positive control: starch and acarbose (0.5 mg kg^{-1}). AgNPs group: starch and AgNPs (1.2 and 2.4 mg kg^{-1}). Blood samples were collected from the tail vein at 0, 15, 30, 60, 90, and 120 minutes after treatment and measured with a glucometer. Data were normalized, and the AUC was calculated using the trapezoidal rule. The antihyperglycemic activity was calculated using eqn (4):

$$\text{Antihiperglycemic activity}\,(\%) = \left(1 - \frac{\text{AUC treatment group}}{\text{AUC water control}}\right) \times 100. \quad (4)$$

Hypoglycemic activity

The hypoglycemic effect was determined according to Uuh–Narvaez *et al.*[25] Six male normoglycemic CD1 mice, without prior fasting, were used. Treatments were administered intraperitoneally: negative control (water, 0.2 mL per 100 g), positive control (insulin, 0.175 mg kg^{-1}; glibenclamide, 0.5 mg kg^{-1}), and AgNPs (0.06 and 12 mg kg^{-1}). Glucose levels were measured from tail vein blood samples using a glucometer. Basal glucose levels were measured before treatment and every hour for 6 hours. The antihyperglycemic activity was calculated using eqn (4) given above.

Statistical analysis

Results were analyzed using descriptive and inferential statistics, expressed as mean ± standard error of the mean (n = 6). A one-way ANOVA followed by Tukey's test was used to assess differences between AgNP samples. In *in vivo* trials, the Dunnett test was used to identify statistical differences

 This journal is © The Royal Society of Chemistry 2026

Open Access Article. Published on 10 December 2025. Downloaded on 1/20/2026 10:49:24 PM. This article is licensed under a Creative Commons Attribution 3.0 Unported Licence.

between formulations and the control group in each experiment. A statistically significant difference was defined as a P value ≤ 0.05. All analyses were conducted using Statgraphics Centurion XV (Manugistics Inc., Rockville, MD, USA) and GraphPad Prism® version 7.00 (GraphPad Software Inc., San Diego, CA, USA).

Results

Inhibition of three enzymes and AGEs

Fig. 1 presents the dose–response curves and inhibitory effects of AgNPs on α-amylase, α-glucosidase, DPP-4 enzymes, and AGE formation. The dotted horizontal line corresponds to 50% inhibition. Panels A, C, E, and G show the determination of inhibitory activity, expressed as the half-maximal inhibitory concentration (IC_{50}), for three enzymes and AGE formation. Panels B, D, F, and H display the quantified IC_{50} values for all AgNP samples and the control across the four evaluated parameters. These graphs demonstrate that all AgNP samples exhibit significantly lower IC_{50} values compared to the control (acarbose, blue lines).

Table 2 also presents the $IC_{50\ control}/IC_{50\ sample}$ ratios, illustrating how many times the activity of the studied sample exceeds that of the control sample, represented by the first-line medicine. The $IC_{50\ control}/IC_{50\ sample}$ ratio varies between 1.8 and 3871.9. The maximum effect of elevated activity was revealed for α-glucosidase $IC_{50\ control}/IC_{50\ sample}$ ratios that lie between 1556.0–3871.9 (Table 2). Therefore, the α-glucosidase inhibition process was of interest to study in more detail. The results of the study of its mechanism will be presented below. Table 1 also shows that Ag2, Ag4, and Ag5 samples demonstrated the highest activity (marked with bold numbers in Table 2) in each of the four studied inhibition processes. So, to find out which sample between the studied ones is optimal, or, in other words, which sample combines quite high activity in all four inhibition processes, the principal component analysis classification was carried out. In addition, the first approximation to shed light on the physicochemical properties determining the optimal activity was made. The results of two of these analyses are also presented below. The data of IC_{50} values calculated from the curves of Fig. 1 are summarized in Table 2.

The mechanisms of inhibition of α-glucosidase activity by AgNPs

Lineweaver–Burk plots and Michaelis–Menten equations were employed through nonlinear regression analysis to evaluate the interaction of AgNPs with α-glucosidase and their impact on its catalytic activity.[26] Fig. 2 presents the Lineweaver–Burk plots, which were used to elucidate the inhibition mechanisms of α-glucosidase by AgNPs.[27] In these plots, the slope corresponds to K_m/V_{max}, while the y-intercept represents $1/V_{max}$.[21]

To determine the inhibition mechanism for each AgNP sample, the parameters of Lineweaver–Burk plots associated with mechanism classification (V_{max} app and K_m app) are presented in Table 3. The kinetic parameter analysis shows that Ag1, Ag2, and Ag3 exhibit a mixed-type inhibition mechanism (Fig. 2A–C), in which the inhibitor binds to both the free enzyme and the enzyme–substrate complex (carbohydrate). This interaction disrupts the effective binding of the substrate and consequently affects product formation.[21] The Michaelis constant (K_m) represents the substrate concentration at which the enzymatic rate reaches half of its maximum value (V_{max}) and reflects the apparent affinity of the enzyme for its substrate. K_m values for four formulations (Ag2, Ag3, Ag4, and Ag5) ranged from 0.9 to 2.4 μg mL^{-1}, except for Ag3, which showed a higher value (4.9 μg mL^{-1}). In contrast, Ag1 exhibited markedly elevated K_m values (8.7 and 10.3 μg mL^{-1}), approximately four times higher than those of the other formulations, indicating a substantially lower affinity for the substrate. Therefore, the lower K_m values of Ag2–Ag5 suggest a higher enzyme–substrate affinity, whereas the increased K_m for Ag1 reflects reduced affinity.

We clarified that the increase in apparent V_{max} observed at low inhibitor concentrations for Ag1 and Ag3 does not contradict classical enzyme kinetics but reflects a mixed-type modulation with a competitive-dominant component ($K_i < K_i'$) and low-dose partial activation. At low concentrations, these PVP-stabilized AgNPs may induce conformational adjustments in the enzyme that transiently enhance catalytic turnover (k_{cat}), while at higher concentrations the inhibitory effect predominates. Ag2 followed a similar mixed-type pattern but without activation, showing a mild decrease in V_{max} accompanied by increased K_m. Conversely, Ag4 and Ag5 demonstrated a competitive inhibition mechanism (Fig. 2D–E), where the inhibitor and the substrate compete directly for the active site. This behavior, like that observed with acarbose,[27] was reflected in a reduction in active site availability for the substrate as the inhibitor concentration increased.[28]

Correlation-based network analysis and classification analysis based on the principal component analysis (PCA)

Current research increasingly uses machine learning (ML) algorithms as key tools for discovering new therapies for neurodegenerative diseases, cancer, stroke, and diabetes.[24] The network analysis based on the correlation between the physicochemical characteristics of AgNP samples and their bioactivities (inhibition of α-amylase, α-glucosidase, DPP-4, and AGEs) is shown in Fig. 3A.

In this study, PCA identified the optimal AgNP sample for inhibiting α-amylase, α-glucosidase, DPP-4, and AGE formation. PC1 and PC2 accounted for 75% and 22% of the variation, with a classification accuracy of 1.0 (Fig. 3B). Ag2 showed the strongest antidiabetic activity, followed by Ag5, while Ag1, Ag3, and Ag4 showed lower activity. PC1 was influenced by hydrodynamic diameter (HD), while PC2 was related to zeta potential (ZP) and size distribution (SD) (Fig. 3C). These results represent the first step in optimizing AgNPs for achieving better antidiabetic effects. Further studies are needed to explore the role of the sample's physicochemical characteristics.

Open Access Article. Published on 10 December 2025. Downloaded on 1/20/2026 10:49:24 PM.
This article is licensed under a Creative Commons Attribution 3.0 Unported Licence.

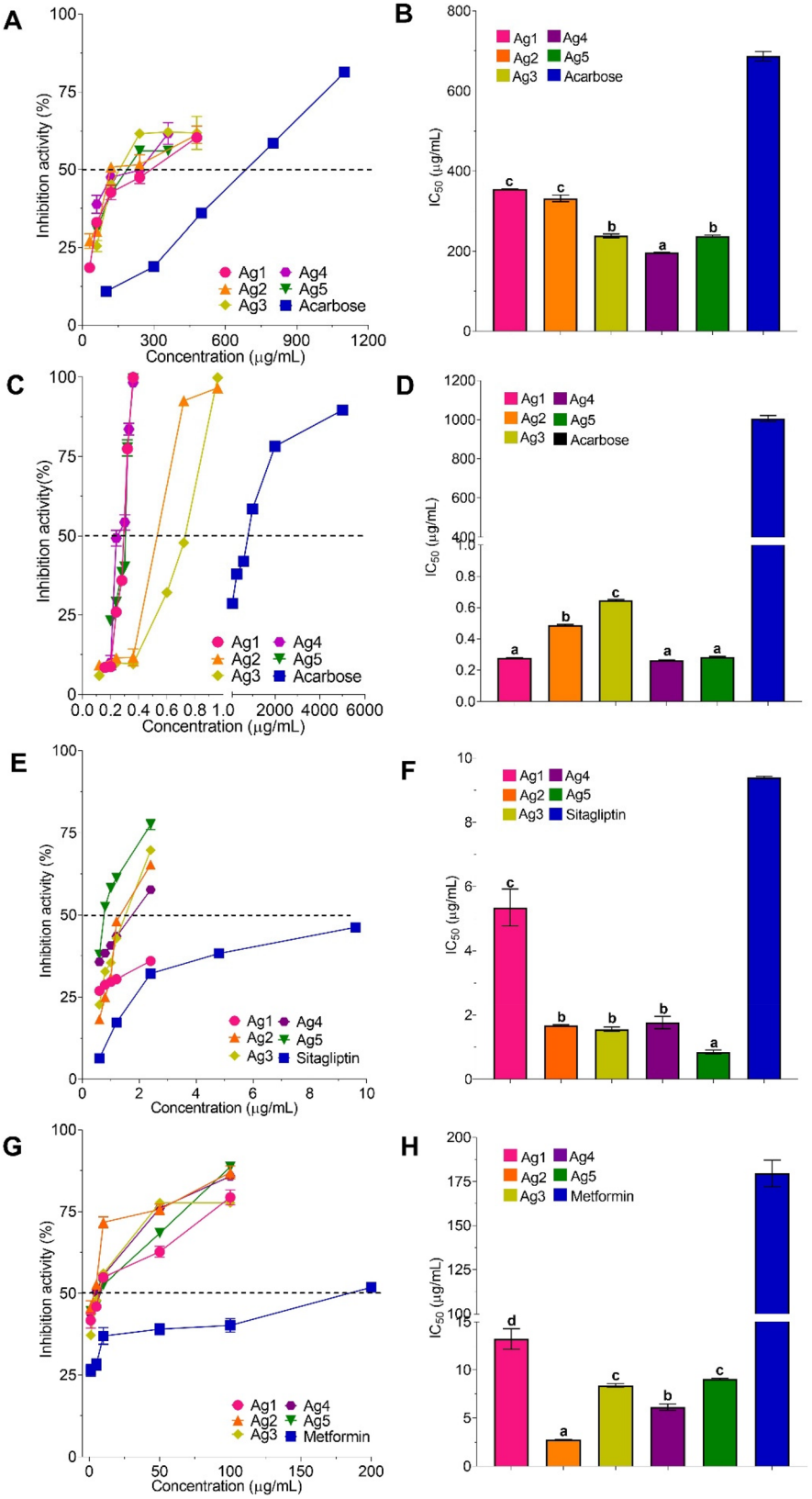

Fig. 1 Dose–response curves and inhibitory effects of AgNPs on α-amylase (A and B), α-glucosidase (C and D), and dipeptidyl peptidase IV (E and F) enzymes and AGE formation (G and H). The black horizontal lines correspond to 50% inhibition. Results are expressed as mean ± SEM of each group (n = 3). Different letter superscripts in the same column of the AgNPs indicate significant difference ($p \leq 0.05$).

This journal is © The Royal Society of Chemistry 2026

Open Access Article. Published on 10 December 2025. Downloaded on 1/20/2026 10:49:24 PM.
This article is licensed under a Creative Commons Attribution 3.0 Unported Licence.

Table 2 IC_{50} values and $IC_{50control}/IC_{50sample}$ ratios for three enzymes and AGEs for five AgNP samples and three control samples

AgNP sample	IC_{50} values, μg mL^{-1} ($IC_{50control}/IC_{50sample}$)			
	α-Amylase	α-Glucosidase	DPP-4	AGEs
Ag1	355.28 ± 0.73 (1.9)	0.27 ± 0.003 (3728.5)	5.35 ± 0.58 (1.8)	13.23 ± 1.07 (13.57)
Ag2	332.05 ± 8.41 (2.1)	0.489 ± 0.004 (2058.7)	1.68 ± 0.02 (5.6)	**2.77 ± 0.01 (64.81)**
Ag3	238.7 ± 4.9 (2.9)	0.648 ± 0.004 (1556.0)	1.56 ± 0.06 (6.0)	8.40 ± 0.17 (21.37)
Ag4	**195.54 ± 1.22 (3.5)**	**0.26 ± 0.004 (3871.9)**	1.77 ± 0.19 (5.3)	6.14 ± 0.33 (29.24)
Ag5	237.9 ± 2.67 (2.9)	0.28 ± 0.004 (3595.4)	**0.85 ± 0.06 (11.1)**	9.07 ± 0.06 (19.79)
Acarbose	686.69 ± 11.68 (1)	1006.7 ± 15.09 (1)	—	—
Sitagliptin	—	—	9.39 ± 0.035 (1)	—
Metformin				179.53 ± 7.59 (1)

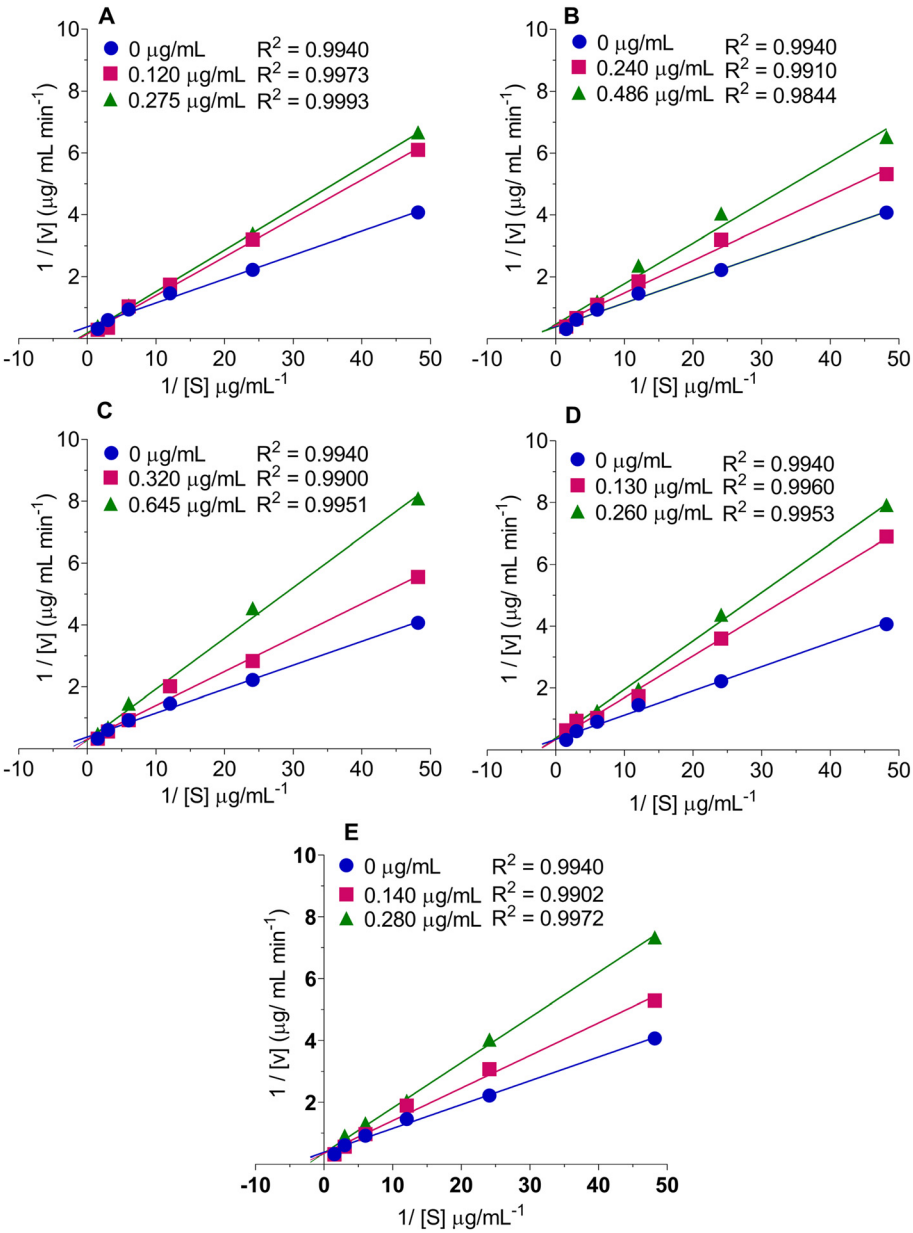

Fig. 2 Lineweaver–Burk plots for α-glucosidase enzyme inhibition (reciprocal of velocity *versus* reciprocal of carbohydrates concentration). A – Ag1. B – Ag2. C – Ag3. D – Ag4 and E – Ag5. Results are expressed as mean ± SEM of each group (n = 3).

Open Access Article. Published on 10 December 2025. Downloaded on 1/20/2026 10:49:24 PM.
This article is licensed under a Creative Commons Attribution 3.0 Unported Licence.

Table 3 Kinetic parameters of α-glucosidase inhibition induced by AgNPs

Sample	Inhibitor concentration (μg mL^{-1})	V_{max} app. (μg mL^{-1} min)	K_m app. (μg mL^{-1})	K_i (μg mL^{-1})	K_i' (μg mL^{-1})	Inhibition type
Ag1	0	2.67 ± 0.05	0.62 ± 0.1	N/A	N/A	Mixed
	0.120	16.64 ± 0.05	10.30 ± 0.09	74.73 ± 0.05	299.40 ± 4.83	
	0.275	12.31 ± 0.03	8.61 ± 0.12	158.93 ± 0.07	590.07 ± 4.63	
Ag2	0	2.67 ± 0.05	0.62 ± 0.01	N/A	N/A	Mixed
	0.240	1.98 ± 0.06	0.84 ± 0.01	177.87 ± 0.12	206.30 ± 3.64	
	0.485	1.71 ± 0.09	1.14 ± 0.01	287.04 ± 0.16	398.33 ± 4.28	
Ag3	0	2.67 ± 0.04	0.62 ± 0.01	N/A	N/A	Mixed
	0.320	4.13 ± 0.06	1.93 ± 0.02	226.45 ± 0.12	397.87 ± 3.95	
	0.640	4.07 ± 0.07	4.71 ± 0.05	302.45 ± 0.15	830.53 ± 14.78	
Ag4	0	2.67 ± 0.04	0.62 ± 0.01	N/A	N/A	Competitive
	0.130	2.88 ± 0.07	2.03 ± 0.06	74.78 ± 0.65	N/A	
	0.260	2.50 ± 0.06	2.40 ± 0.05	128.38 ± 0.20	N/A	
Ag5	0	2.67 ± 0.04	0.62 ± 0.01	N/A	N/A	Competitive
	0.140	2.85 ± 0.07	1.23 ± 0.0	102.94 ± 0.05	N/A	
	0.280	2.79 ± 0.03	2.31 ± 0.0	148.59 ± 0.07	N/A	

V_{max} app – apparent value of maximum velocity in the presence of the inhibitor, K_m app – apparent value of Michaelis–Menten constant in the presence of the inhibitor, K_i – inhibition constant, K_i': inhibition constant of the ES complex, N/A: cases when is not possible to determine the constant for the type of inhibition shown, since as it can only be calculated in the case of mixed inhibition.

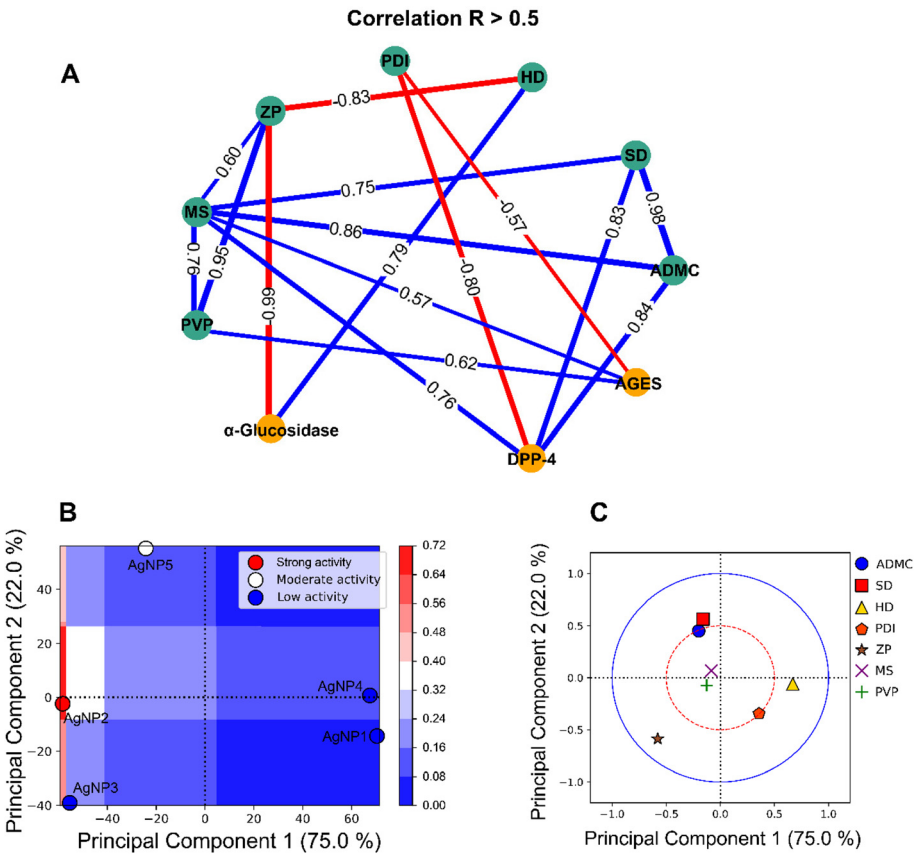

Fig. 3 Correlation network analysis between biological activities and physicochemical properties of AgNPs (A). Principal component analysis load plot (B and C). PVP: polyvinylpyrrolidone concentration, MS: metallic silver concentration, ZP: zeta potential, PDI: polydispersity index, HD: hydrodynamic diameter, SD: size distribution, ADMC: average diameter of metallic cores, AGEs: advanced glycation end-products, DPPIV: dipeptidyl peptidase IV.

In Table 4 the multivariate AgNP activity classification based on the IC_{50} values of bioactivities with setting the AgNP formulation with maximum activity as the reference sample (100% activity) is presented.

Table 4 and Fig. 3B illustrate that the Ag2 sample belongs to the high activity category (>50% in four bioactivities, bold numbers in Table 4), Ag5 to the moderate activity (>50% in three bioactivities), and Ag1, Ag3, and Ag4 to the low activity

This journal is © The Royal Society of Chemistry 2026

Open Access Article. Published on 10 December 2025. Downloaded on 1/20/2026 10:49:24 PM. This article is licensed under a Creative Commons Attribution 3.0 Unported Licence.

Table 4 The multivariate AgNP activity classification (taking the AgNP formulation with maximum activity as the reference sample of 100% activity)

AgNP sample	$IC_{50\ control}/IC_{50\ sample}$ (percentage relative to reference sample activity)			
	α-Amylase	α-Glucosidase	DPP-4	AGEs
Ag1	**1.9 (54.3%)**	**3728.5 (96.3%)**	1.8 (16.2%)	12.9 (21.0%)
Ag2	**2.1 (60.0%)**	**2058.7(53.2%)**	**5.6 (50.5%)**	**61.4 (100%)**
Ag3	**2.9 (82.9%)**	1556.0 (40.2%)	**6.0 (54.1%)**	20.2 (32.95)
Ag4	**3.5 (100%)**	**3871.9 (100%)**	5.3 (47.7%)	27.7 (45.1%)
Ag5	**2.9 (82.9%)**	**3595.4 (92.9%)**	**11.1 (100%)**	18.8 (30.6%)

Bold numbers correspond to >50% in four bioactivities.

category (>50% in two bioactivities). Fig. 3A illustrates a complicated net of positive and negative correlations between physicochemical parameters and bioactivities and between physicochemical parameters themselves.

In the present study, both antihyperglycemic and hypoglycemic effects were investigated. The first experiment evaluated the antihyperglycemic effect, defined as the inhibition of the glycemic peak 30 minutes after starch administration in rats. This assessment aimed to determine the capacity of the tested samples to attenuate the rise in blood glucose levels following a carbohydrate load. The hypoglycemic effect refers to the decrease in normal blood glucose levels in healthy mice.

AgNP anti-hyperglycemic potential: OGTT in healthy rats

The results of the anti-hyperglycemic activity for animal groups treated with various AgNP samples at doses of 1.2 and 2.4 mg kg^{-1}, as well as for the control group treated with acarbose, are depicted in Fig. 4. Starch administration increased plasma glucose levels, reaching maximum hyperglycemia 30 minutes after administration, with a normalized value for glucose of 1.24 ± 0.09. In contrast, acarbose administration inhibited the activity of α-glucosidases, resulting in a 15.71 ± 4.49% reduction in starch hydrolysis, if the hyperglycemic peak induced by starch administration was accepted as 100% (Fig. 4B). At a dose of 1.2 mg kg^{-1}, Ag2 (11.01 ± 1.95%), Ag4 (10.31 ± 14.05%), and Ag5 (14.05 ± 1.91%) effectively inhibited the hyperglycemic peak, with no significant differences compared to acarbose ($P \leq 0.05$) (Fig. 4B).

For glucose regulation, the AUC was calculated. Acarbose showed irreversible inhibition of glucose homeostasis at 12.35 ± 4.10% (Fig. 4C). Among the AgNPs, Ag5 exhibited irreversible homeostasis regulation at 8.0 ± 1.48% (1.2 mg kg^{-1} dose, Fig. 4C), with no significant difference compared. Ag2 and Ag4, however, showed reversible inhibition, with increased glucose absorption at 45 and 45–60 minutes, resulting in regulation measures of 5.66 ± 1.82% and 3.24 ± 2.59%, respectively (Fig. 4C). At 2.4 mg kg^{-1}, all AgNPs inhibited hyperglycemia (Fig. 4D), with Ag2 showing the highest inhibition (6.73 ± 2.46%) (Fig. 4E). Ag1 and Ag3 did not inhibit glucose significantly at 30 minutes but reduced glucose levels at 45 minutes, suggesting delayed absorption. Overall, Ag2 (2.4 mg kg^{-1}) and Ag5 (1.2 mg kg^{-1}) showed homeostasis regulation comparable to acarbose.

Hypoglycemic effect in normoglycemic rats

Fig. 5 illustrates the hypoglycemic activity of AgNPs samples administered at doses of 0.06 mg kg^{-1} and 12.0 mg kg^{-1} to mouse groups. These results were compared to control groups receiving insulin (0.174 mg kg^{-1}), glibenclamide (10 mg kg^{-1}), and water (0.2 mL per 100 g body weight). The AgNPs doses (0.06 and 12.0 mg kg^{-1}) were significantly lower and higher, respectively, than those used in the antihyperglycemic activity study (1.2 and 2.4 mg kg^{-1}, as shown in Fig. 4). The selected sharply different AgNP doses allowed us to make a first approximation over a wide dose range.

Fig. 5 and Table 5 present the results of the hypoglycemic activity of AgNP formulations and two controls. Insulin administration significantly reduced glucose levels, decreasing by 55.30 ± 1.32% at 60 minutes and achieving an overall glucose regulation of 26.56 ± 5.08% (Fig. 5A). In contrast, the control group treated with glibenclamide (10 mg kg^{-1}) exhibited a gradual decline in glucose levels, achieving an overall regulation of 6.95 ± 2.84% without a pronounced hypoglycemic peak at 60 minutes (Fig. 5B). The analysis AUC (Fig. 5B) indicated that AgNP formulations Ag2, and Ag3 (0.06 mg kg^{-1}) produced hypoglycemic effects comparable to glibenclamide, showing no significant differences, there by demonstrated a relative potency approximately 167 times greater than glibenclamide. Ag1, Ag3, and Ag5 (12 mg kg^{-1}) achieved the same hypoglycemic effect as glibenclamide (10 mg kg^{-1}) (Fig. 5D). None of the AgNP formulations at doses of 0.06 or 12 mg kg^{-1} reached the hypoglycemic peak achieved with insulin (55.30% at 0.17 mg kg^{-1}).

Discussion

Table 2 presents the IC_{50} values of AgNP samples (Ag1–Ag5), which are 1.9–3.5, 1556.0–3871.9, 1.8–11.1, and 12.9–61.4 times lower than acarbose (for α-amylase inhibition), acarbose (for α-glucosidase inhibition), sitagliptin (for DPP-4 inhibition), and metformin (for AGE inhibition), respectively. Table S1 (SI) compares the IC_{50} values for inhibiting α-amylase, α-glucosidase, DPP-4, and AGE formation across different AgNP formulations, controls, and extracts from previous and present studies. While most research focuses on α-amylase and α-glucosidase inhibition, fewer studies explore

Open Access Article. Published on 10 December 2025. Downloaded on 1/20/2026 10:49:24 PM.
This article is licensed under a Creative Commons Attribution 3.0 Unported Licence.

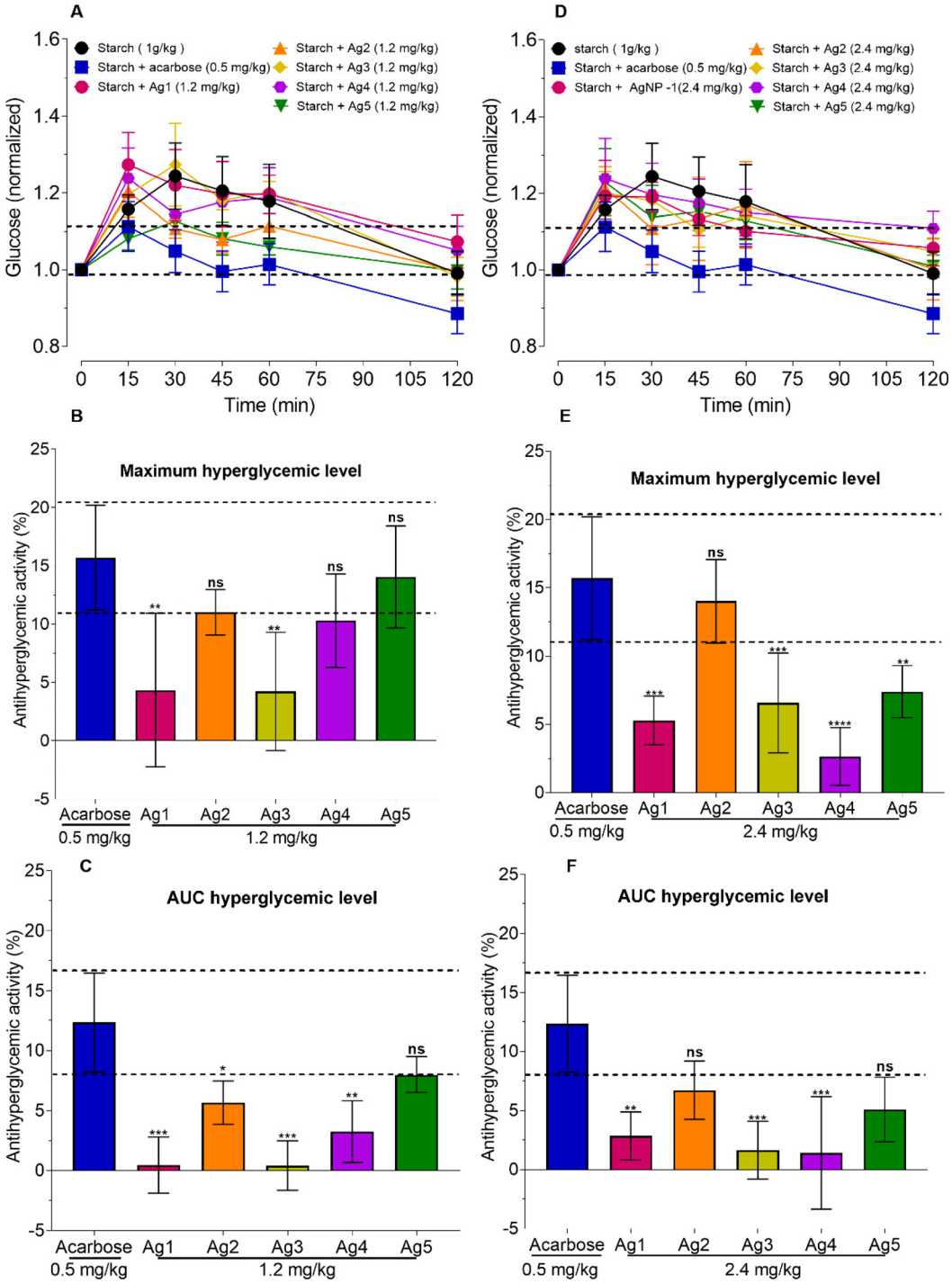

Fig. 4 Antihyperglycemic activity of AgNP formulations at doses 1.2 (A–C) and 2.4 mg kg^{-1} (D–F) and acarbose at doses 0.5 mg kg^{-1} in healthy rats. Kinetic antihyperglycemic activity (A and D), maximum hyperglycemic levels (at 30 minutes) (B and E), and AUC hyperglycemic levels (C and F). Results are expressed as mean ± SEM of each group (n = 6). Data were analyzed using ANOVA and Dunnett's *post hoc* test. *$P \leq 0.05$ compared to the acarbose-treated group. Ns: no significant statistical differences.

DPP-4 inhibition, and we couldn't find IC_{50} data for AGE inhibition.

In Table S1, literature data for 20 AgNP formulations [1–14, SI] were compared with the results of our five AgNP formulations. Among the 20 AgNP formulations studied previously, the results for AgNP obtained from plant extracts dominate, although there are two AgNP formulations obtained from biological compound derivatives and two obtained by chemical synthesis. The AgNP formulations from the first group (including data for 13 AgNP formulations from 9 first publications

This journal is © The Royal Society of Chemistry 2026

Open Access Article. Published on 10 December 2025. Downloaded on 1/20/2026 10:49:24 PM. This article is licensed under a Creative Commons Attribution 3.0 Unported Licence.

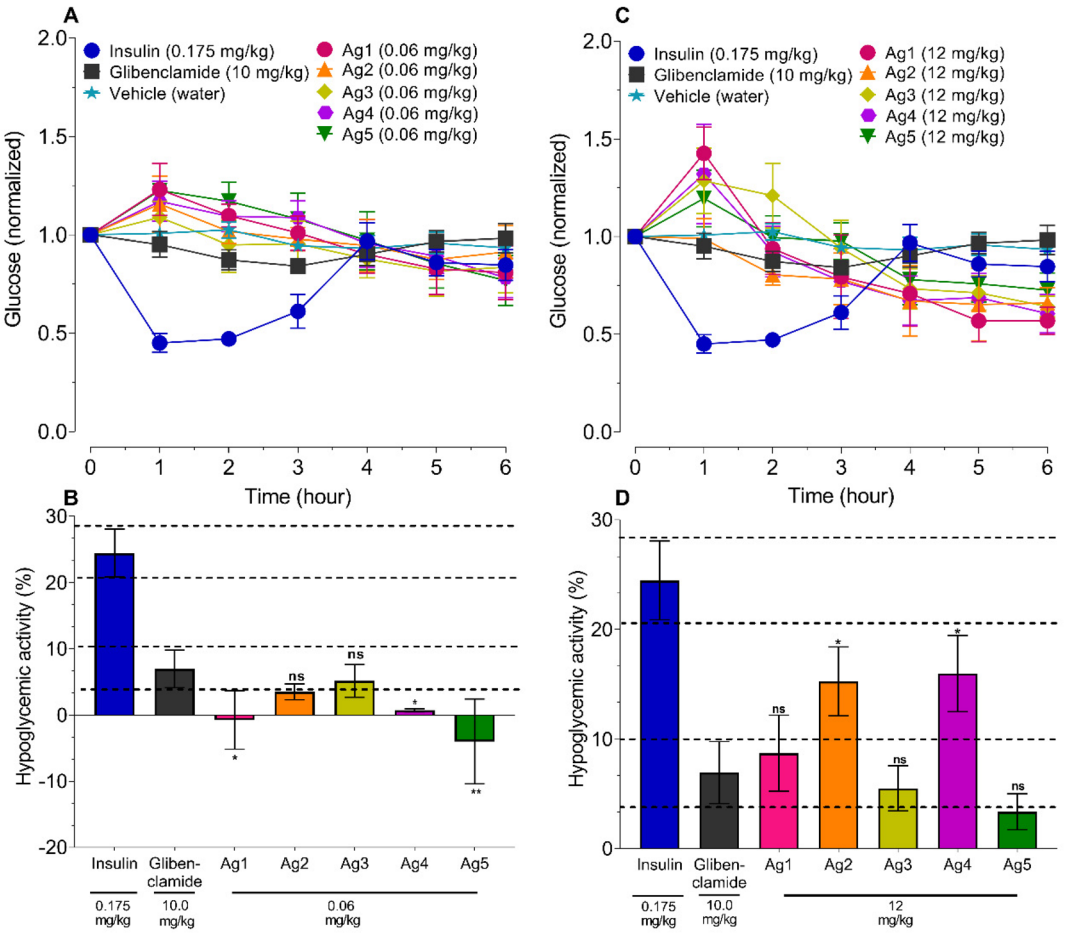

Fig. 5 Hypoglycemic activity of AgNP formulations at doses 0.06 (A and B) and 12 mg kg^{-1} (C and D). Change of blood glucose levels with time (A and C) and the percentage of hypoglycemic activity (B and D). Results are expressed as mean ± SEM of each group (n = 6). Data were analyzed using ANOVA and Dunnett's *post hoc* test. *$P \leq 0.05$ compared to the glibenclamide-treated group. Ns: no significant statistical differences.

Table 5 Antihyperglycemic and hypoglycemic activities of AgNP formulations and controls

Sample	Antihyperglycemic activity (%)				Hypoglycemic activity (%) for two doses	
	Maximum hyperglycemic level (30 min) for two different doses		Hyperglycemic level AUC for two different doses			
	1.2 mg kg^{-1}	2.4 mg kg^{-1}	1.2 mg kg^{-1}	2.4 mg kg^{-1}	0.06 mg kg^{-1} AUC	12.0 mg kg^{-1} AUC
Ag1	4.34 ± 6.58	5.29 ± 1.79	0.45 ± 2.35	2.85 ± 2.04	−0.73 ± 4.91	8.72 ± 3.48
Ag2	11.01 ± 1.95	14.02 ± 3.06	5.66 ± 1.82	6.73 ± 2.46	3.50 ± 1.19	15.27 ± 3.14
Ag3	4.22 ± 5.06	6.57 ± 3.67	0.41 ± 2.07	1.64 ± 2.45	5.15 ± 3.16	5.51 ± 2.07
Ag4	10.31 ± 4.0	2.64 ± 2.12	3.24 ± 2.59	−1.27 ± 4.98	0.75 ± 0.24	15.99 ± 3.48
Ag5	14.05 ± 1.91	7.41 ± 1.91	8.0 ± 1.48	5.09 ± 2.74	−3.99 ± 6.05	3.38 ± 1.65
Interval for Ag1–Ag5	4.22–14.05	2.64–14.02	0.41–8.0	−1.27–6.73	−3.09–5.15	3.38–15.99
Average for Ag1–Ag5	8.79	7.19	3.55	3.00	0.94	9.77
Acarbose, 500 mg kg^{-1}	15.71 ± 4.49		12.35 ± 4.10		—	—
Glibenclamide, 10 mg kg^{-1}	—	—	—	—	6.95 ± 2.84	
Insulin, 0.174 mg kg^{-1}	—	—	—	—	24.49 ± 3.59	

listed in Table S1) are not of significant interest for further consideration, as they were less effective than the existing antidiabetic medications (controls). In contrast, the AgNPs formulations of the second group (including data from 7 AgNPs formulations from 5 previous publications and 5 AgNP formulations from the present study) demonstrated superior activity,

Open Access Article. Published on 10 December 2025. Downloaded on 1/20/2026 10:49:24 PM. This article is licensed under a Creative Commons Attribution 3.0 Unported Licence.

with IC_{50} values lower than those of the controls. In the second group, only one AgNP formulation (AgNPs/*Annona muricata*) demonstrated the $IC_{50\ sample}/IC_{50\ control}$ ratio higher than that of our AgNP formulations.[29] AgNPs/*A. muricata* was 32.4 times more effective in α-amylase inhibition but 21 times less effective in α-glucosidase inhibition and slightly less effective in DPP-4 inhibition than our top-performing AgNP samples. However, AgNPs derived from plant extracts, like *A. muricata*, present inherent challenges. These include extract instability in solutions and uncontrollable variations in chemical composition due to factors such as light, humidity, soil composition, and the presence of microorganisms. Moreover, natural products face technical hurdles in the isolation, characterization, and standardization of active components, which limit their appeal for pharmaceutical development.

In contrast, the controlled synthesis of Argovit™ AgNPs, used in this study, offers a significant advantage in consistency and reliability over plant-based AgNP formulations. Polymer coatings have a significant impact on nanoparticle efficiency by enhancing colloidal stability, preventing aggregation, modifying surface charge, stabilizing nanoparticles in biological fluids, altering cell interactions, controlling drug release, and improving biosensing sensitivity through mechanisms such as fluorescence quenching suppression and plasmonic enhancement.[30,31] Bare nanoparticles are often limited by uncontrolled aggregation and a lack of stability, which polymer coatings can mitigate, leading to improved performance in biomedical and other applications.[32] PVP as a nanoparticle coating has advantages. It is a non-toxic water-soluble synthetic polymer widely used in the pharmaceutical, cosmetic, and food industries.[33] In the Argovit™ formulations, the PVP coating ensures homogeneity, maintains nanoparticle dispersion, and prevents unwanted interactions with biomolecules, which collectively enhance their biological activity and safety.

When considering alternatives to first-line anti-diabetic drug, few substances have demonstrated greater potential. Recent studies have highlighted the search for potent α-glucosidase inhibitors due to their key role in glucose regulation. Of 1275 compounds reviewed,[34–36] only two surpassed the AgNPs evaluated here. Among the reported compounds, the coordination compound synthesized by from 1,10-phenanthroline and mercury acetate showed a relative potency of 5962.73 times higher than the acarbose control. However, mercury (Hg) content makes it unsuitable for treatment due to toxicity concerns.[37] Another, a bis-indolylmethane derivative, was 8560 times more potent than acarbose but had issues with synthesis, yield, and cost.[38] These challenges make large-scale use of plant derivatives impractical. In contrast, Argovit™ AgNP formulations offer a more feasible, consistent, and scalable alternative for diabetes treatment.

In vitro, AgNP formulations studied here inhibit DPP-4 (IC_{50}: 0.85–5.34 μg mL^{-1}), suggesting their potential to enhance insulin secretion and suppresses glucagon-mediated glycogenolysis. Argovit™ AgNPs demonstrate potential in diabetes management by inhibiting DPP-4, regulating glucose, preventing AGE formation, and inhibiting α-glucosidase. Animal studies further confirmed their hypoglycemic potential: AgNPs administered at doses comparable to acarbose and 167 times lower than glibenclamide achieved similar antihyperglycemic effects. This suggests that AgNPs could reduce the required doses of conventional drugs, lowering toxicity and side effects.

The consistent behavior of all Argovit™ AgNP formulations indicates that PVP-stabilized AgNPs represent a robust class of multifunctional nanotherapeutics capable of targeting multiple diabetic pathways simultaneously. However, while the enzyme inhibition and *in vivo* responses are promising, additional studies—such as insulin and glucose tolerance tests, redox balance analysis, and chronic exposure assays—are required to further validate their therapeutic potential and elucidate the molecular mechanisms involved.

Finally, it is essential to highlight the favorable safety profile of Argovit AgNPs. In our previous work,[11] the lethal doses (LD_{50}) of the five Argovit™ formulations studied here were determined with oral administration on mice. This study was performed according to OECD Guideline 420 for the Acute Oral Toxicity Assay on mice. $DL50_{Ag}$ calculated for metallic Ag for all five formulations are in the interval 1067–1.806 mg kg^{-1} and placed them in Category 4 of the Globally Harmonized System of Classification and Labelling of Chemicals.[11] The DL50 calculated for AgNPs (metallic Ag together with the stabilizer) is 16.67 times greater than $DL50_{Ag}$ (17 783–30 100 mg kg^{-1}), which places them in the "harmless" classification (≫5.000 mg kg^{-1}). The oral LD_{50} of glibenclamide in mice is around 3250 mg kg^{-1},[39] which means that $LD_{50\ AgNPs}$ is 5.5–9.2 times higher than $LD_{50\ glibenclamide}$. Histopathological analysis revealed that the accumulation of AgNPs primarily occurs in the gastrointestinal system, without significant damage to the exposed tissue.[11] Argovit AgNPs are not genotoxic at the doses applied for mouse melanoma treatment.[12] Moreover, at 100 mg kg^{-1}, they have genoprotective properties decreasing genotoxic damage caused by anticancer drugs 2–4 times (and arabinose and cyclophosphamide).[13,14] They are neither cytotoxic nor genotoxic to the ambient and can be used as fertilizers at low concentrations.[40] Hemolysis of healthy and diabetic human erythrocytes[15] and human lymphocytes[16] caused by Argovit™ AgNPs was lower than that caused by other AgNP formulations. Numerous essays on humans, such as prevention of SARS-CoV-2,[17] treatment of diabetic foot,[18] treatment of tuberculosis of the upper respiratory tract,[19] application after nasal cavity and paranasal sinuses surgery,[20] further support their safety for biomedical use.

Conclusion

It was revealed that *in vitro* experiments, Argovit™ AgNPs exhibited effectiveness in the inhibition of three enzymes possessing a great impact in diabetic treatment: α-amylase, α-glucosidase, and DPP-4 up to 3.51, 3827.76, and 11 times higher than the inhibition effectiveness of the first-line anti-

 This journal is © The Royal Society of Chemistry 2026

Open Access Article. Published on 10 December 2025. Downloaded on 1/20/2026 10:49:24 PM. This article is licensed under a Creative Commons Attribution 3.0 Unported Licence.

diabetic drugs acarbose and sitagliptin. Moreover, inhibition of the formation of advanced glycation end products by AgNPs was up to 61.4 times higher than that of the first-line antidiabetic drug metformin. The increase in α-glucosidase inhibition effectiveness up to 3827.76 suggests that these AgNP formulations act as very potent inhibitors under the tested conditions. The high effectiveness of AgNPs in inhibiting four processes was promising for the development of innovative antidiabetic drugs.

In vivo research revealed that AgNP antihyperglycemic activity was comparative to the activity of acarbose. While the same hypoglycemic effect was achieved with AgNP doses up to 167 times lower than that of glibenclamide. This substantial decrease in required glibenclamide doses suggests that AgNP use could reduce the toxicity and side effects associated with conventional antidiabetic treatments, highlighting the need for further research to confirm their potential as an antidiabetic drug.

This study provides preliminary data regarding the potential application of Argovit™ AgNPs formulation for treating Type 2 diabetes mellitus. Additional systematic experiments, long-term toxicity assessments, and clinical trials are required.

Author contributions

Conceptualization – JJAF, MRSC, VVP, NB, and AP, methodology – MRSC, JJAF, and VVP, software – AAP, validation – VVP, AAP, JJAF, MRSC, and NB, formal analysis – AAP, investigation – JJAF and VVP, resources – JJAF, NB, MRSC and AP, data curation – NB, VVP, JJAF, MRSC, and AP, writing – original draft – VVP, MRSC, NB and AAP, writing – review & editing – VVP, NB, and MRSC, visualization – VVP and AAP, supervision – JJAF, MRSC, NB, and AP. Project administration – JJAF and MRSC. Funding acquisition – JJAF, MRSC, and NB.

Conflicts of interest

The authors declare that there are no relationships or conflict of interest that might bias their research.

Data availability

The datasets generated and/or analysed during the current study are available in the GitHub repository: https://github.com/antadlp/agnps-antidiabetic-data-analysis. All data supporting the findings of this study are openly available under the license specified in the repository.

Supplementary information (SI) is available. See DOI: https://doi.org/10.1039/d5nr03452c.

Acknowledgements

The authors thank Fundación UNAM A.C., Mexico (Project "International Network of Bionanotechnology" No. 311.06.101) and the Program of the Ministry of Education and Science of the Russian Federation (Project No. 075-03-2025-439/2) for their financial support.

References

1 M. A. Díaz-Román, J. J. Acevedo-Fernández, G. Ávila-Villarreal, E. Negrete-León and A. B. Aguilar-Guadarrama, Phytochemical analysis and antihyperglycemic activity of Castilleja arvensis, *Fitoterapia*, 2024, **174**, 105839, DOI: 10.1016/j.fitote.2024.105839.

2 J. J. Uuh-Narváez, M. A. González-Tamayo and M. R. Segura-Campos, A study on nutritional and functional study properties of Mayan plant foods as a new proposal for type 2 diabetes prevention, *Food Chem.*, 2021, **341**, 128247, DOI: 10.1016/j.foodchem.2020.128247.

3 J. J. U. Narváez, *et al.*, Metabolic profile of *Psidium guajava* L. fruits and their inhibitory mechanisms against α-amylase and α-glucosidase, *Fitoterapia*, 2025, **185**, 106781, DOI: 10.1016/j.fitote.2025.106781.

4 M. A. Marzouk, E. M. Mahmoud, W. S. Shehab, S. M. Fawzy, S. M. Mohammed, M. A. Abdel-Razek, G. E. Khedr and D. A. Elsayed, Dual α-amylase and α-glucosidase inhibition by 1,2,4-triazole derivatives for diabetes treatment, *Sci. Rep.*, 2025, **15**, 27172, DOI: 10.1038/s41598-025-11214-4.

5 P. Routabi, M. Mehrabi, H. Adibi, M. Mehrabi and R. Khodarahmi, Design and evaluation of curcumin-derived aldopentose compounds: Unlocking their antidiabetic potential through integrative *in vitro*, *in vivo*, and *in silico* studies on carbohydrate-degrading enzymes, *J. Nutr. Biochem.*, 2025, **141**, 109897, DOI: 10.1016/j.jnutbio.2025.109897.

6 P. Xu, X. Yang and Y. Wang, Inhibition of non-enzymatic glycation by capsaicin: targeting AGE-induced diabetic complications, *New J. Chem.*, 2021, **45**(35), 16048–16058, DOI: 10.1039/D1NJ01783G.

7 S. S. Kulabas, H. Ipek, A. R. Tufekci, *et al.*, Ameliorative potential of Lavandula stoechas in metabolic syndrome via multitarget interactions, *J. Ethnopharmacol.*, 2018, **223**, 88–98, DOI: 10.1016/j.jep.2018.04.043.

8 J. S. Hussein, W. Rasheed, T. Ramzy, *et al.*, Synthesis of docosahexaenoic acid–loaded silver nanoparticles for improving endothelial dysfunctions in experimental diabetes, *Hum. Exp. Toxicol.*, 2019, **38**(8), 962–973, DOI: 10.1177/0960327119843586.

9 N. Masood, R. Ahmed, M. Tariq, *et al.*, Silver nanoparticle impregnated chitosan-PEG hydrogel enhances wound healing in diabetes induced rabbits, *Int. J. Pharm.*, 2019, **559**, 23–36, DOI: 10.1016/j.ijpharm.2019.01.019.

Open Access Article. Published on 10 December 2025. Downloaded on 1/20/2026 10:49:24 PM. This article is licensed under a Creative Commons Attribution 3.0 Unported Licence.

10 C. A. A. Hernandez, R. L. Vazquez-Gomez, D. Garibo-Ruiz, R. A. L. V. Gomez, I. V. Vega, H. Almanza-Reyes, A. Pestryakov and N. Bogdanchikova, Nanomedicine approach for the rapid healing of diabetic foot ulcers with silver nanoparticles, *J. Clin. Med. Images*, 2020, **3**(2), 1–7.

11 O. U. Cruz-Ramírez, L. M. Valenzuela-Salas, A. Blanco-Salazar, *et al.*, Antitumor activity against human colorectal adenocarcinoma of silver nanoparticles: Influence of [Ag]/[PVP] ratio, *Pharmaceutics*, 2021, **13**(7), 1000, DOI: 10.3390/pharmaceutics13071000.

12 L. M. Valenzuela-Salas, N. G. Girón-Vázquez, J. C. García-Ramos, O. Torres-Bugarín, C. Gómez, A. Pestryakov, *et al.*, Antiproliferative and antitumour effect of nongenotoxic silver nanoparticles on melanoma models, *Oxid. Med. Cell. Longevity*, 2019, **2019**, 4528241, DOI: 10.1155/2019/4528241.

13 I. Y. Castañeda-Yslas, O. Torres-Bugarín, J. C. García-Ramos, Y. Toledano-Magaña, P. Radilla-Chávez, N. Bogdanchikova, *et al.*, AgNPs Argovit™ modulates cyclophosphamide-induced genotoxicity on peripheral blood erythrocytes in vivo, *Nanomaterials*, 2021, **11**(8), 2096, DOI: 10.3390/nano11082096.

14 I. Y. Castañeda-Yslas, O. Torres-Bugarín, M. E. Arellano-García, B. Ruiz-Ruiz, J. C. García-Ramos, Y. Toledano-Magaña, *et al.*, Protective effect of silver nanoparticles against cytosine arabinoside genotoxicity: an in vivo micronucleus assay, *Int. J. Environ. Res. Public Health*, 2024, **21**(12), 1689, DOI: 10.3390/ijerph21121689.

15 R. Luna-Vázquez-Gómez, M. E. Arellano-García, J. C. García-Ramos, P. Radilla-Chávez, D. S. Salas-Vargas, F. Casillas-Figueroa, *et al.*, Hemolysis of human erythrocytes by Argovit™ AgNPs from healthy and diabetic donors: an in vitro study, *Materials*, 2021, **14**(11), 2792, DOI: 10.3390/ma14112792.

16 B. Ruiz-Ruiz, M. E. Arellano-García, P. Radilla-Chávez, D. S. Salas-Vargas, Y. Toledano-Magaña, F. Casillas-Figueroa, *et al.*, Cytokinesis-block micronucleus assay using human lymphocytes as a sensitive tool for AgNPs cytotoxicity/genotoxicity evaluation, *ACS Omega*, 2020, **5**(21), 12005–12015, DOI: 10.1021/acsomega.0c00149.

17 H. Almanza-Reyes, I. Plascencia-López, M. Alvarado-Vera, L. Patrón-Romero, A. Reyes-Escamilla, D. Valencia-Manzo, *et al.*, Effect of mouthwash and nose rinse with silver nanoparticles for the prevention of SARS-CoV-2 infection in health workers, *PLoS One*, 2021, **16**(8), e0256401, DOI: 10.1371/journal.pone.0256401.

18 C. A. A. Hernandez, R. L. Vazquez-Gomez, D. Garibo-Ruiz, R. A. L. V. Gomez, I. V. Vega, H. Almanza-Reyes, A. Pestryakov and N. Bogdanchikova, Nanomedicine approach for the rapid healing of diabetic foot ulcers with silver nanoparticles, *J. Clin. Med. Images*, 2020, **3**(2), 1–7.

19 B. B. Uraskulova and A. O. Gyusan, Clinical and bacteriological study of the effectiveness of the use of silver nanoparticles for the treatment of tuberculosis of the upper respiratory tract, *Vestn. Otorinolaringol.*, 2017, **82**(3), 54–57, DOI: 10.17116/otorino201782354-57.

20 K. M. Fidarova and F. V. Semenov, The topical application of Ag nanoparticles based medications after the nasal cavity and paranasal sinuses surgery, *Russ. Otorhinolaryngol.*, 2016, (3), 147–151, DOI: 10.18692/1810-4800-2016-3-147-151.

21 B. Dineshkumar, A. Mitra and M. Mahadevappa, Antidiabetic and hypolipidemic effects of mahanimbine (carbazole alkaloid) from Murraya koenigii (rutaceae) leaves, *Int. J. Phytomed.*, 2010, **2**(1), 22–30, DOI: 10.5138/ijpm.2010.0975.0185.02004.

22 L. Kan, E. Capuano, V. Fogliano, *et al.*, Inhibition of α-glucosidases by tea polyphenols in rat intestinal extract and Caco-2 cells grown on Transwell, *Food Chem.*, 2021, **361**, 130047, DOI: 10.1016/j.foodchem.2021.130047.

23 M. Starowicz and H. Zieliński, Inhibition of advanced glycation end-product formation by high antioxidant-leveled spices commonly used in European cuisine, *Antioxidants*, 2019, **8**(4), 100, DOI: 10.3390/antiox8040100.

24 T. Srisongkram, S. Waithong, T. Thitimetharoch and N. Weerapreeyakul, Machine learning and in vitro chemical screening of potential α-amylase and α-glucosidase inhibitors from Thai indigenous plants, *Nutrients*, 2022, **14**, 347, DOI: 10.3390/nu14020267.

25 J. J. Uuh-Narvaez, E. Negrete-León, J. J. Acevedo-Fernández and M. R. Segura-Campos, Antihyperglycemic and hypoglycemic activity of Mayan plant foods in rodent models, *J. Sci. Food Agric.*, 2021, **101**(10), 4193–4200, DOI: 10.1002/jsfa.11057.

26 S. A. Saganuwan, Application of modified Michaelis – Menten equations for determination of enzyme inducing and inhibiting drugs, *BMC Pharmacol. Toxicol.*, 2021, **22**, 57, DOI: 10.1186/s40360-021-00521-x.

27 H. U. Son and S. H. Lee, Comparison of α-glucosidase inhibition by Cudrania tricuspidata according to harvesting time, *Biomed. Rep.*, 2013, **1**(4), 624–628, DOI: 10.3892/br.2013.111.

28 R. Copeland, Reversible modes of inhibitor interactions whith enzymes, in *Evaluation of Enzyme Inhibitors in Drug Discovery: A Guide for Medicinal Chemists and Pharmacologists (Chap. 3, second Edition)*, 2013, pp. 20–65.

29 J. A. Badmus, S. A. Oyemomi, O. T. Adedosu, *et al.*, Photo-assisted bio-fabrication of silver nanoparticles using Annona muricata leaf extract: exploring the antioxidant, anti-diabetic, antimicrobial, and cytotoxic activities, *Heliyon*, 2020, **6**(11), e05413, DOI: 10.1016/j.heliyon.2020.e05413.

30 R. Kato, M. Uesugi, Y. Komatsu, F. Okamoto, T. Tanaka, F. Kitawaki and T.-A. Yano, Highly stable polymer coating on silver nanoparticles for efficient plasmonic enhancement of fluorescence, *ACS Omega*, 2022, **7**(5), 4286–4292, DOI: 10.1021/acsomega.1c06010.

31 A. M. Iureva, P. I. Nikitin, E. D. Tereshina, M. P. Nikitin and V. O. Shipunova, The influence of various polymer coatings on the in vitro and in vivo properties of PLGA nanoparticles:

 This journal is © The Royal Society of Chemistry 2026

Open Access Article. Published on 10 December 2025. Downloaded on 1/20/2026 10:49:24 PM.
This article is licensed under a Creative Commons Attribution 3.0 Unported Licence.

Comprehensive study, *Eur. J. Pharm. Biopharm.*, 2024, **201**, 114366, DOI: 10.1016/j.ejpb.2024.114366.

32 F. Perreault, A. Oukarroum, S. P. Melegari, W. G. Matias and R. Popovic, Polymer coating of copper oxide nanoparticles increases nanoparticles uptake and toxicity in the green alga *Chlamydomonas reinhardtii*, *Chemosphere*, 2012, **87**(11), 1388–1394, DOI: 10.1016/j.chemosphere.2012.02.046.

33 F. Perreault, A. Oukarroum, S. P. Melegari, W. G. Matias and R. Popovic, Polymer synthesis and processing, in *Natural and synthetic biomedical polymers*, Elsevier, 2014, pp. 1–31. DOI: 10.1016/B978-0-12-396983-5.00001-6.

34 A. Singh, K. Singh, A. Sharma, *et al.*, Recent developments in synthetic α-glucosidase inhibitors: A comprehensive review with structural and molecular insight, *J. Mol. Struct.*, 2023, **1281**, 135115, DOI: 10.1016/j.molstruc.2023.135115.

35 A. Mushtaq, U. Azam, S. Mehreen and M. M. Naseer, Synthetic α-glucosidase inhibitors as promising anti-diabetic agents: Recent developments and future challenges, *Eur. J. Med. Chem.*, 2023, **249**, 115119, DOI: 10.1016/j.ejmech.2023.115119.

36 T.-P. Lam, N.-V. N. Tran, L.-H. D. Pham, *et al.*, Flavonoids as dual-target inhibitors against α-glucosidase and α-amylase: a systematic review of in vitro studies, *Nat. Prod. Bioprospect.*, 2024, **14**(1), 4, DOI: 10.1007/s13659-023-00424-w.

37 Y.-S. Wu, A. I. Osman, M. Hosny, *et al.*, The Toxicity of Mercury and Its Chemical Compounds: Molecular Mechanisms and Environmental and Human Health Implications: A Comprehensive Review, *ACS Omega*, 2024, **9**(5), 5100–5126, DOI: 10.1021/acsomega.3c07047.

38 M. Gollapalli, M. Taha, H. Ullah, *et al.*, Synthesis of Bis-indolylmethane sulfonohydrazides derivatives as potent α-Glucosidase inhibitors, *Bioorg. Chem.*, 2018, **80**, 112–120, DOI: 10.1016/j.bioorg.2018.06.001.

39 X. Serrano-Martín, G. Payares and A. Mendoza-León, Glibenclamide, a blocker of K + ATP channels, shows anti-leishmanial activity in experimental murine cutaneous leishmaniasis, *Antimicrob. Agents Chemother.*, 2006, **50**(12), 4214–4216, DOI: 10.1128/AAC.00617-06.

40 F. Casillas-Figueroa, M. E. Arellano-García, B. Ruiz-Ruiz, R. Luna Vázquez-Gómez, P. Radilla-Chávez, R. A. Chávez-Santoscoy, *et al.*, Cytotoxic and genotoxic effects of silver nanoparticles on Allium cepa: similar story, totally different outcome, *Nanomaterials*, 2020, **10**(7), 1386, DOI: 10.3390/nano10071386.